Beni-Suef University Journal of Basic and Applied Sciences

RESEARCH

Open Access

Assessment of single and combined administration of ubiquinone and lactoferrin on histopathology, ultrastructure, oxidative stress, and WNT4 expression gene induced by thioacetamide on hepatorenal system of adult male rats

Sohaila Abd El-Hameed[1*], Iman Ibrahim[1], Walaa Awadin[1] and Ahmed El-Shaieb[1]

Abstract

Background Hepatorenal syndrome is a life-threatening medical complication of liver cirrhosis. Hepatic cirrhosis is commonly accompanied by rapid failure of renal functions. Thioacetamide (TAA) is a potent hepatotoxin and a class 2-type carcinogen. Ubiquinone (Coq_{10}) and lactoferrin (LF) are potent antioxidants with antifibrotic and antiinflammatory effects. However, whether Coq_{10} and LF reduce the hepatorenal injury induced by TAA remains unclear. Here, we investigated the potential protective effect of both/or Coq_{10} and LF in ameliorating TAA-induced hepatorenal injury and the role of WNT4 gene expression in detecting TAA-induced renal injury in rats. Seventy healthy and mature male Sprague Dawley rats, weighting (200 g ± 20 g) and aging (4–6) weeks were randomly divided into seven groups ($n = 10$): control, Coq_{10}, LF, TAA, TAA + Coq_{10}, TAA + LF, and TAA + Coq_{10} + LF. The hepatorenal injury was induced through intraperitoneal (i.p.) injection of TAA (150 mg/kg/twice/weekly) for nine weeks. Coq_{10} (10 mg/kg/day) and LF (200 mg/kg/day) were orally administered for nine weeks.

Results TAA induced marked hepatorenal damage, evident by the significant increase in the alanine aminotransferase (ALT), aspartate transaminase (AST), serum creatinine (SCr) activities, and the blood urea nitrogen (BUN) level. Besides, the significant increases in concentrations of malondialdehyde (MDA) and nitric oxide (NOx) together with significant decreases in the activities of catalase (CAT) and superoxide dismutase (SOD). The histopathological analysis of the TAA group showed obvious fibrosis, steatosis, and inflammation of the hepatic parenchyma as well as severe glomerular and tubular damage of the renal parenchyma. In addition, TAA induced marked ultrastructural alterations and up-regulation in the expression of the WNT4 gene in the kidney. Meanwhile, the biochemical, histopathological, and ultrastructural alterations were significantly decreased with significant down-regulation in the expression of WNT4 in the groups exposed to TAA and treated with Coq_{10} and LF.

Conclusion Our data suggested that Coq_{10} and LF could have protective effects on TAA hepatorenal damage, through improving the hepatic and renal functions, reduction of oxidative stress, structural and ultrastructural alterations, besides down-regulation in the expression of WNT4.

Keywords Ubiquinone, Lactoferrin, Thioacetamide, Hepatorenal injury, Histopathology, Ultrastructural, WNT4

*Correspondence:
Sohaila Abd El-Hameed
drsohailaabdelhameed@mans.edu.eg; sohaila.abdelhamid@yahoo.com
Full list of author information is available at the end of the article

1 Background

Hepatic fibrosis is a worldwide public health problem that fallouts in hepatic cirrhosis, cancer, and death [1]. Hepatorenal syndrome is a special type of renal impairment in patients suffering from hepatic cirrhosis [2]. This renal insufficiency is induced by splanchnic vasodilatation followed by consecutive renal vasoconstriction [3]. This splanchnic vasodilatation is due to the over-generation and release of the vasodilators in the splanchnic circulation, resulting in systemic vasodilation [4]. Systemic vasodilation decreases the effective blood volume and the systemic pressure in the arteries, including the renal arteries [5].

Thioacetamide (TAA) is a known industrial compound that is used in laboratory and industrial applications, including metallurgy, fungicides, and pesticides pharmaceuticals [6]. It is a source of sulfide ions in various chemical industries [7]. Experimentally, TAA is regarded as the ideal toxin to induce hepatic fibrosis and cirrhosis [8]. TAA itself is inert; it is bioactivated in the liver to give thioacetamide S-oxide, which generates peroxide radicals and produces reactive oxygen species (ROS) [6]. ROS initiates oxidation reactions, including lipid peroxidation and protein denaturation, leading to liver injury [9].

The kidneys are highly sensitive to lipid peroxidation and oxidative stress owing to their richness in long polyunsaturated fatty acids and their filtration of large amounts of toxins that could be concentrated in the renal tissues [10]. The responses of the kidney to toxicants varied by numerous morphological patterns, starting with tubular or interstitial changes to nephropathy [11]. However, the exact mechanisms of kidney function problems during chronic liver diseases or cirrhosis induced by TAA are poorly understood, necessitating further investigations to identify novel protective or protective approaches for the management of this condition.

The WNT4 gene is a member of a family of 19 genes that play critical roles in the renal developmental processes before birth [12]. They offer instructions and the chemical signaling pathways that regulate the interactions between cells during embryonic development and are hushed in the normal adult kidneys [13]. The expression of WNT4 is re-activated in certain renal pathological conditions; therefore, it is the chief biomarker of kidney diseases [14].

Ubiquinone, or coenzyme Q_{10} (Coq_{10}), is a vitamin-like substance and a necessary cofactor of the respiratory chain [15]. It is a main constituent in the mitochondria of eukaryotes [16]. It is a potent antioxidant with anti-inflammatory activities that protect the cell from injurious insults [17]. It is broadly consumed as a dietary supplement to increase the bioenergetic power and to slow certain pathological conditions [18, 19].

Lactoferrin (LF) is an iron-binding glycoprotein that exists in most biological fluids, with high levels in mammalian milk "colostrum" [20]. It is excreted in the saliva, semen, tears, vaginal fluids, bile, gastrointestinal fluids, and bronchial secretions [21]. LF is synthesized and released by neutrophils and mucosal epithelial cells in numerous mammalian species, e.g., humans, cattle, horses, goats, and dogs [22]. It belongs to the transferrin and has a variety of biological activities, including inhibiting pro-inflammatory pathway activation, tissue damage, and sepsis [23]. Therefore, this study aimed to understand the mechanism of renal damage secondary to TAA-induced hepatic cirrhosis, the role of the WNT4 gene in detecting this renal damage, and the protective mechanism of both/or Coq_{10} and LF on TAA hepatorenal damage.

2 Methods

2.1 Chemicals and drugs

Thioacetamide was obtained from Oxford Lab Chemicals, India, dissolved in sterile distilled water, and prepared as a fresh solution for intraperitoneal (i.p.) injection. Coq_{10} was purchased from Sigma-Aldrich (St. Louis, USA), dissolved in sterile physiological saline (0.9 NaCl) containing 1% Tween 80 (*v/v*), and prepared as a fresh solution for oral administration. LF was obtained from the lactoferrin CO (NSW, Australia), dissolved in distilled water, and freshly prepared for oral administration.

2.2 Animals

Seventy healthy and mature male Sprague Dawley rats, weighing 200 g ± 20 g, aging (4–6) weeks were kept in plastic cages under standard humane and hygienic conditions, including temperature (25˚C) and light with 12 h light/dark cycle. This research is approved by the Medical Research Ethics Committee of Mansoura University at the April 11, 2021, Code No, Ph.D, 85.

2.3 Experimental design

The rats were kept for two weeks as an adaptation period; then, they were randomly divided into seven groups (ten rats/each).

The first: (control group), the rats were reared under standard conditions and received no treatments.

The second: (Coq_{10} group), the rats received a daily oral dose of Coq_{10} (10 mg/kg) for nine weeks [24].

The third: (LF group), the rats received a daily oral dose of LF (200 mg/kg) for nine weeks [25].

The fourth: (TAA group), the rats received an i.p. dose of TAA (150 mg/kg/twice/weekly) for nine weeks [26].

The fifth: (TAA + Coq_{10} group), the rats received an i.p. dose of TAA (150 mg/kg/twice/weekly) and a daily oral dose of Coq_{10} (10 mg/kg) for nine weeks.

The sixth: (TAA + LF group), the rats received an i.p. dose of TAA (150 mg/kg/twice/weekly) and a daily oral dose of LF (200 mg/kg) for nine weeks.

The seventh: (TAA + Coq_{10} + LF group), rats received an i.p. dose of TAA (150 mg/kg/twice/weekly), daily oral doses of Coq_{10} (10 mg/kg) and LF (200 mg/kg) for nine weeks.

2.4 Serum biochemical analysis

One day after the last treatment with TAA, Coq_{10}, and LF, and under thiopental sodium anesthesia (20 mg/kg), blood was drawn from the retro-orbital vein in sterile serum tubes. The serum separation took place via blood centrifugation at 4000 rounds/minute for 10 min. The serum samples were used for estimation of alanine aminotransferase (ALT), aspartate transaminase (AST), and serum creatinine (SCr) activities as well as the blood urea nitrogen (BUN) level using specific kits from Diamond Diagnostics and Spectrum Diagnostics, Egypt [27, 28].

2.5 Oxidative stress and antioxidant markers

After the blood samples were collected, the rats were killed via cervical dislocation. The evisceration of the liver and kidneys took place immediately. Then, the liver and kidneys were rinsed in ice-cooled physiological saline. After that, a weighted part of each liver and kidney was homogenized with phosphate buffered saline, followed by centrifugation at 4000 rounds/minute for 10 min. The homogenates were used for the assessment of malondialdehyde (MDA) and nitric oxide (NOx) concentrations as well as catalase (CAT) and superoxide dismutase (SOD) activities using specific kits from Biodignostic, Egypt [29, 30].

2.6 Histopathological and scoring systems

Representative hepatic and renal tissues were well preserved in 10% neutral buffered formalin for two days for perfect fixation. Then, the samples were washed with water, dehydrated with alcohol, and embedded in paraffin wax. After that, each section was cut at a thickness of four µm using a rotatory microtome (MNC-2 microtome, USSR) and deparaffinized with xylene. Finally, each section was stained either by hematoxylin and eosin (H&E) or by Masson's trichrome stain (MTC) [31]. Three tissue sections were taken from each group, and four fields were examined/each (3X4 = 12 field). The sections were examined by light microscopy (XSZ-107BN biological microscope, China) and photographed by sc30 Olympus camera for detection of any pathological changes. The histopathological scores were calculated according to the data in Tables 1 and 2 [32, 33].

2.7 Transmission electron microscopy (TEM)

Representative renal samples were preserved in cold glutaraldehyde (4%), washed in cacodylate, postfixed in OsO4(1%), washed in buffer, dehydrated with alcohol, and embedded in a mixture of aepon and araldite according to the technique of E.M. Unit, Assiut University [34]. From the blocks, semi-thin sections were prepared at a thickness of 0.5–1 µm using an LKB ultra-microtome, and stained with toluidine. After that, ultra-thin sections were made at a thickness of 500–700 Å using a Leica AG ultra-microtome. The sections were examined by a JEM 100 CXII electron microscope at 80 kV and photographed by a CCD digital camera, Model XR- 41.

Table 1 Histopathological scoring of hepatic parenchyma

Score	Apoptosis (0–4)	Steatosis (0–4)	Fibrosis (0–4)	Inflammation (0–4)
0	None	None	None	None
1 (Minimal)	Field showed 1–2 apoptotic cells	Field exhibited focal microvesicular steatosis	Field exhibited portal fibrosis	Field showed occasional one inflammatory foci
2 (Mild)	Field showed 3–4 apoptotic cells	Field exhibited diffuse microvesicar steatosis	Field exhibited portal fibrosis with thin short non-anastomosing collagen bundles	Field showed periportal inflammatory cell infiltration
3 (Moderate)	Field showed 5–6 apoptotic cells	Field exhibited micro- to macrovesicar steatosis	Field exhibited septal fibrosis with formation of incomplete cirrhotic nodules, no obvious cirrhosis	Field showed diffuse portal inflammatory cell infiltration
4 (Severe)	Field showed 7–8 apoptotic cells	Field exhibited diffuse macrovesicular steatosis with prominent signet ring appearance	Field exhibited septal fibrosis, complete cirrhotic nodules with obvious cirrhosis	Field showed diffuse portal and septal inflammatory cell infiltration

Table 2 Histopathological scoring of renal parenchyma

Score	Tubular damage (0–4)	Glomerular damage (0–4)	Fibrosis (0–4)
0	None	None	None
1 (Minimal)	Field exhibited occasional degenerative changes only	Field exhibited glomerular degeneration and inflammation	Field showed focal replacement of the renal parenchyma by thin collagen bundles
2 (Mild)	Field exhibited degenerative changes with inflammation	Field exhibited glomerular atrophy	Field showed diffuse replacement of the renal parenchyma by thin collagen bundles
3 (Moderate)	Field exhibited degenerative changes with necrosis of the renal tubular epithelium and inflammation	Field exhibited glomerular shrinkage and inflammation	Field showed focal replacement of the renal parenchyma by thick collagen bundles
4 (Severe)	Field exhibited degenerative changes with diffuse necrotizing interstitial nephritis	Field exhibited glomerular shrinkage, inflammation, necrosis, thickening and lamellar fusion	Field showed diffuse replacement of the renal parenchyma by thick collagen bundles

Table 3 Method of the PCR Master Mix preparation

Constituent	Volume (µl)/ reaction
2 × HERA SYBR® Green RT-qPCR Master Mix	10
RT Enzyme Mix (20X)	1
Forward primer (20 pmol)	0.5
Reverse primer (20 pmol)	0.5
Water	5
Template RNA	3
Total	20

2.8 WNT4 gene

Renal samples were collected in Eppendorf tubes, covered with RNA later, and stored at -20˚C.

2.8.1 Extraction of ribonucleic acid (RNA)

The RNA was extracted using a QIAamp RNeasy Mini kit (Qiagen, Germany, GmbH). The steps of the RNA extraction were applied according to the instructions of the kit. The sample (200 µl) was added to the RLT buffer (600 µl) containing mercaptoethanol (10 µl/1 ml), and incubated at 25°C for 10 min. Then, the cleared lysate was treated with one volume of ethanol (70%).

2.8.2 SYBR green reverse transcription polymerase chain reaction (RT-PCR)

The primers were purchased from Metabion in Germany, while the *HERA* SYBR® Green RT-qPCR Master Mix was purchased from Willowfort in the UK. The rat *B-actin* and WNT4 primer sequences were designed and verified by the gene bank [35, 36]. The Primers were utilized in a total reaction of 20-µl, according to the *HERA* SYBR Green PCR kit. The method of the PCR Master Mix preparation was detailed in Table 3. A step one real-time PCR machine was used for the reaction. The sequences of primers and the PCR cycling conditions according to the *HERA* SYBR Green PCR kit were recorded in Table 4.

2.8.3 Analysis of the RT-PCR results

The step one Stratagene MX3005P software was used to determine the amplification curves and Ct values. For the estimation of the differences in gene expression on RNA

Table 4 Primer sequences, amplicon sizes, and cycling conditions for SYBER green RT-PCR

Target gene	Primers sequences	Reverse transcription	Primary denaturation	Amplification (40 cycles)		
				Secondary denaturation	Annealing (Optics on)	Extension
B- actin	TCCTCCTGAGCGCAA GTACTCT	50 °C 30 min	94 °C 15 min	94˚C 15 s	60 °C 30 s	72 °C 30 s
	GCTCAGTAACAGTCC GCCTAGAA					
WNT4	ATGGAGCCGATCCGG TCCAG					
	CACCATGCACCTCTC CCAGC					

in different samples, the Ct value of each sample was compared with that of the positive control group according to the "ΔΔCt" method stated by [37].

2.9 Statistical analysis

The data were analyzed using one-way (ANOVA) with Tukey's test for group comparison [38]. The hypothesis was depending on the difference between groups ($p \leq 0.05$). The statistical analysis was applied using GraphPad software, version, 5 [39].

3 Results

3.1 Ubiquinone (Coq_{10}) and lactoferrin (LF) improve TAA-induced hepatorenal dysfunction

To assess the protective efficacy of Coq_{10} and LF in ameliorating TAA-induced hepatorenal injury, ALT, AST, ALP, SCr, and BUN were measured in the serum.

The serum ALT, AST, and SCr activities as well as the BUN level were significantly increased in the TAA group compared with the control group. The activities of ALT, AST, SCr, and BUN level were significantly decreased in the TAA + Coq_{10} and TAA + LF groups compared with the TAA group, but still significantly different from the control group. The serum hepatic and renal parameters were maintained at normal levels in the TAA + Coq_{10} + LF group compared with the control group (Fig. 1).

3.2 Ubiquinone (Coq_{10}) and lactoferrin (LF) reduce TAA-induce oxidative stress and improve antioxidant

To investigate the protective efficacy of Coq_{10} and LF against TAA-induced oxidative stress, oxidative stress markers (MDA and NOx) and antioxidants (CAT and SOD) were measured in the liver and kidney.

3.2.1 Oxidative parameters (MDA and NOx)

The TAA group showed significant increases in the hepatic and renal concentrations of MDA and NOx compared with the control group. The hepatic and renal concentrations of MDA and NOx were significantly decreased in the TAA + Coq_{10} and TAA + LF groups compared with the TAA group, but still significantly different from the control group. Meanwhile, TAA + Coq_{10} + LF group recorded significant decreases in the hepatic and renal oxidative markers from the TAA group and nonsignificant increases from the control group (Fig. 2).

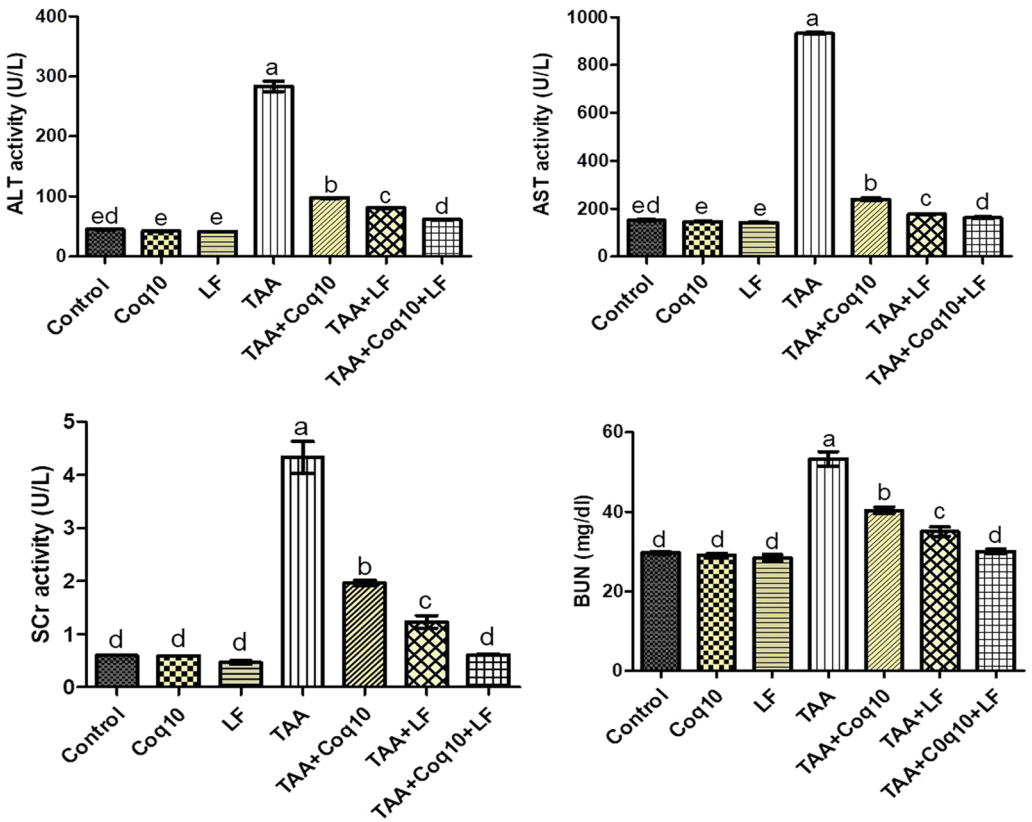

Fig. 1 Effect of TAA, Coq_{10}, and LF on serum parameters (ALT and AST and SCr and BUN) in the studied groups: mean ± SEM, means with different letters indicate a significant difference ($P \leq 0.05$), SEM = standard error of the mean

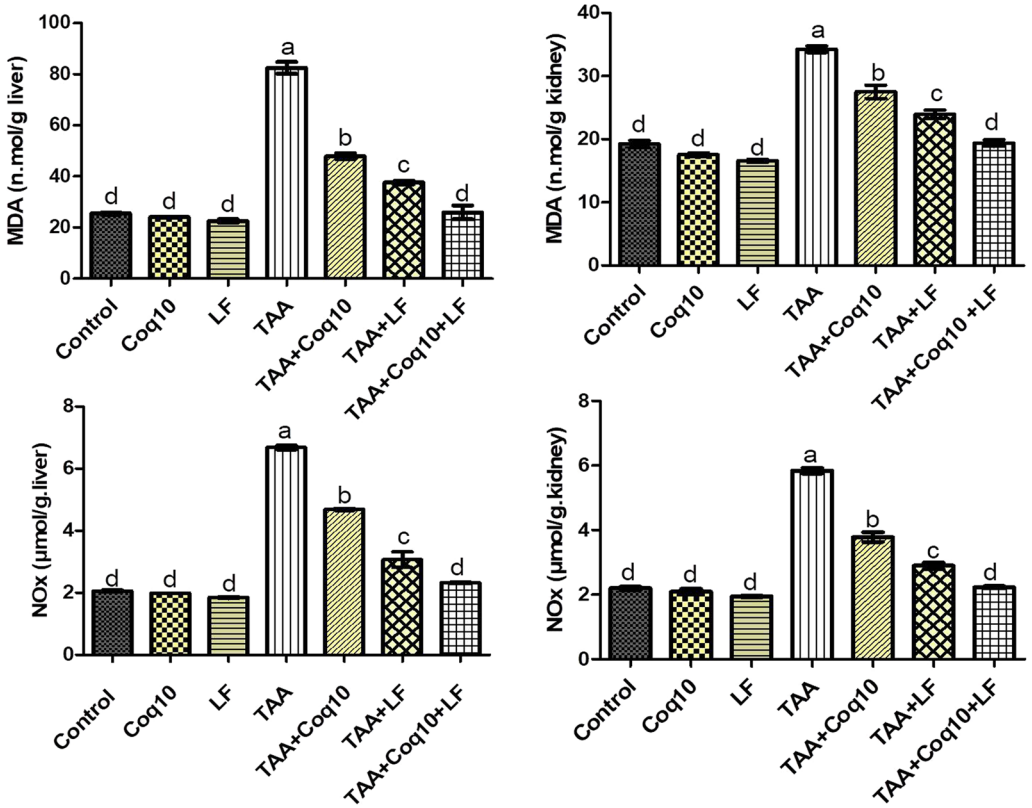

Fig. 2 Effect of TAA, Coq_{10}, and LF on oxidative markers (MDA and NOx) in the studied groups: mean ± SEM, means with different letters indicate a significant difference ($P \leq 0.05$), SEM = standard error of the mean

3.2.2 Antioxidants (CAT and SOD)

The hepatic and renal activities of CAT and SOD were significantly decreased in the TAA group compared with the control group. The TAA + Coq_{10} and TAA + LF groups recorded significant increases in the hepatic and renal activities of CAT and SOD from TAA group and significant decreases from the control group. However, TAA + Coq_{10} + LF group showed a significant increase in the hepatic and renal antioxidant markers from the TAA group and a nonsignificant decrease from the control group (Fig. 3).

3.3 Ubiquinone (Coq_{10}) and lactoferrin (LF) reduce TAA-induced hepatorenal histopathological damage

In order to evaluate the protective effects of LF and Coq_{10} against TAA-induced hepatorenal dysfunction, histopathological examinations of the hepatic and renal sections were recorded following exposure to TAA.

The hepatic alterations were significantly increased in the TAA group compared with the control group and the other experimental groups ($p \leq 0.05$) (Fig. 4H).

In the hepatic sections, normal hepatic parenchyma with normally arranged hepatic cords, normal portal areas, and sinusoids were seen in the control, Coq_{10}, and LF groups (Fig. 4A–C).

The TAA group showed dense fibrous septa separated and divided the hepatic parenchyma into multiple cirrhotic nodules, infiltrated with mononuclear cells, many apoptotic bodies together with hyperchromasia, small cell-type dysplastic cells with eosinophilic intranuclear inclusion, mitotic figures, and macrovesicular steatosis (Fig. 4D1–D5). Conversely, the hepatic parenchyma was divided into incomplete hepatic nodules by thin fibrous septa infiltrated with mononuclear cells, and congested blood vessels were seen in the TAA + Coq_{10} group. Additionally, Moderate microvesicular steatosis was also observed (Fig. 4E). TAA + LF group exposed portal fibrosis with short fibrous tissue extensions, containing few mononuclear cells and mild microvesicular steatosis (Fig. 4F), while TAA + Coq_{10} + LF group showed minimal portal fibrosis infiltrated with few mononuclear cells and mild microvesicular steatosis (Fig. 4G).

The MTC stained hepatic sections signified no fibrous deposition in hepatic parenchyma around the portal areas in control, Coq_{10}, and LF groups (Fig. 5A–C). TAA group showed thickened fibrous bridges dividing the hepatic parenchyma into separate various-sized

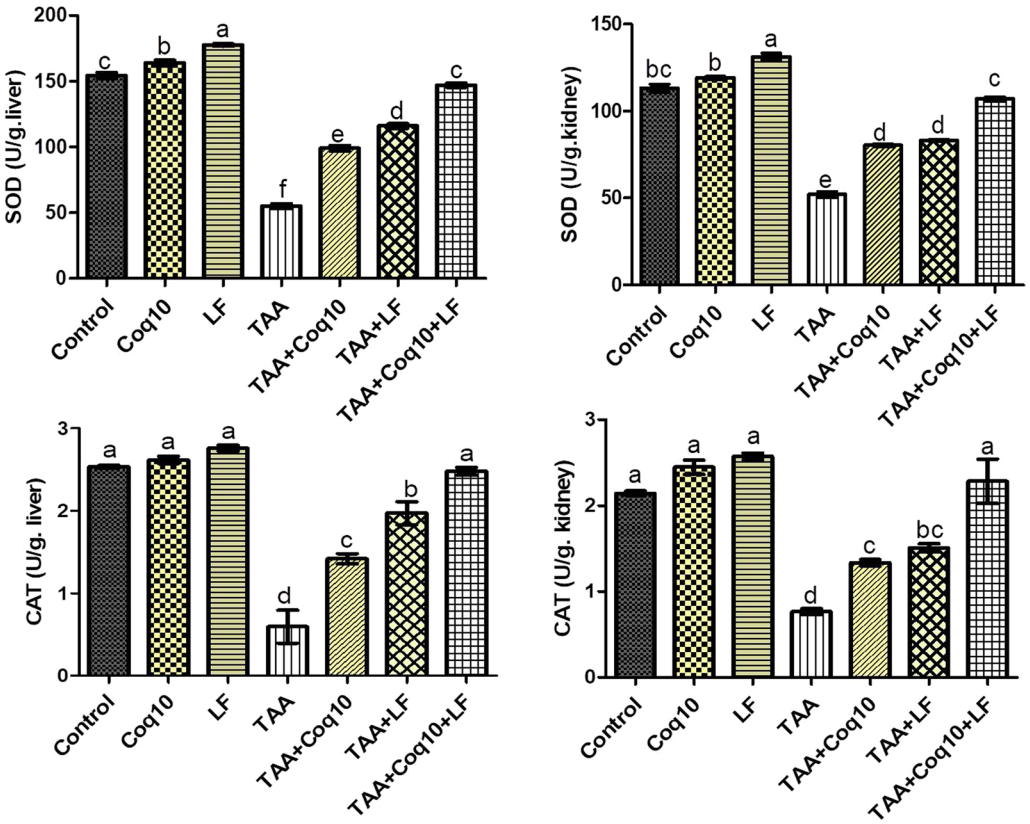

Fig. 3 Effect of TAA, Coq_{10}, and LF on antioxidative markers (CAT and SOD) in the studied groups: mean ± SEM, means with different letters indicate a significant difference ($P \leq 0.05$), SEM = standard error of the mean

nodules (Fig. 5D1–D3). In contrast, TAA + Coq_{10} group revealed deposition of thick non-anastomosing fibrous septa mainly in the portal area (Fig. 5E). Additionally, thin anastomosing portal fibrous septa were obviously seen in the TAA + LF group (Fig. 5F). TAA + Coq_{10} + LF group showed a clear decrease in the positive fibrotic portal area with a very thin and very short non-anastomosing fibrous extension (Fig. 5G). The renal alterations were significantly increased in TAA group compared with control group and the other experimental groups ($P \leq 0.05$) (Fig. 6H).

Normal renal parenchyma, normal renal tubules, and glomeruli were observed in control, Coq_{10}, and LF groups (Fig. 6A–C). The renal sections of the TAA group showed perivascular fibrosis and edema, diffuse ballooning degeneration, and coagulative necrosis of tubular epithelial lining (Fig. 6D1, D2). Additionally, the glomeruli are atrophied, shrunken, necrotic, and crescent in shape with thickened basement membrane (Fig. 6D3–D5). On the other hand, TAA + Coq_{10} group showed moderate hydropic degeneration of the tubular lining epithelium in a few tubules and dilated Bowman's space (Fig. 6E). TAA + LF group recorded mild tubular dilation and dilated Bowman's space (Fig. 6F). TAA + Coq_{10} + LF group signified marked improvement of the histological picture of tubules and glomeruli with normalized Bowman's space (Fig. 6G).

The renal sections stained by MTC recorded no collagen fiber deposition in the renal parenchyma of control, Coq_{10}, and LF groups (Fig. 7A–C). Marked deposition of thick bluish collagen bundles in the renal parenchyma was revealed in TAA group (Fig. 7D1–D3). Meanwhile, TAA + Coq_{10} group showed lower bluish collagen deposition in renal parenchyma and decrease in the deposition of the bluish collagen (Fig. 7E). TAA + LF group showed mild bluish collagen bundles in the renal parenchyma (Fig. 7F). TAA + Coq_{10} + LF group showed no collagen deposition in the renal parenchyma (Fig. 7G).

3.4 Ubiquinone (Coq_{10}) and lactoferrin (LF) reduce TAA-induced renal ultrastructural changes

The ultrastructural examination of the renal tissues was done to investigate the mechanism of hepatorenal injury following TAA exposure and to confirm the histopathological findings.

The TEM micrographs of the renal tubules from control, Coq_{10}, and LF groups revealed normal tubules with normal ultrastructures of nucleus, mitochondria, rough

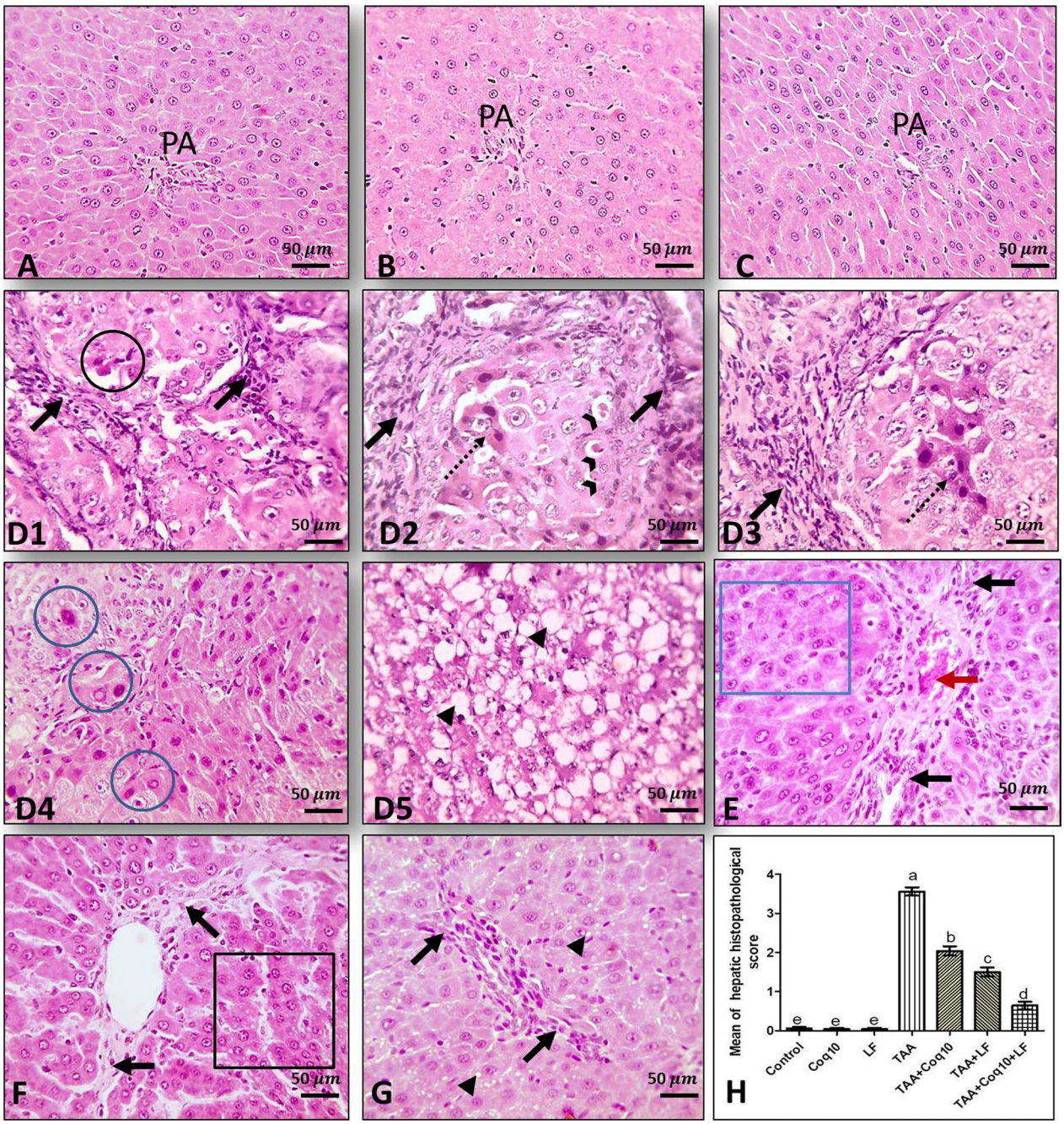

Fig. 4 Representative photomicrographs of hepatic sections from different experimental groups: **A**–**C** showing normal hepatic parenchyma with normal radially arranged hepatic cords, normal portal area (PA) in control, Coq_{10}, and LF groups, respectively. **D1**–**D5** TAA group, showing thick fibrous septa, infiltrated with mononuclear cells (black arrows) separated and divided the hepatic parenchyma into complete cirrhotic nodules. The hepatocytes of the cirrhotic nodules are showing apoptosis (opened arrowheads), marked dysplasia with hyperchromasia (dashed arrow), small cell-type dysplastic cells with eosinophilic intranuclear inclusion (blue circles), mitotic figures (black circle), and diffuse severe macrovesicular steatosis with prominent signet ring appearance (closed arrowhead). **E** TAA + Coq_{10} group, showing fibrous septa infiltrated with mononuclear cells partially divided the hepatic parenchyma into incomplete nodules(black arrows) together with congested blood vessels (red arrow) and moderate microvesicular steatosis of the hepatic parenchyma (blue Square). **F** TAA + LF, showing mild portal fibrosis with short fibrous tissue extensions, containing some mononuclear cells (black arrows) and few hepatocytes appearing with microvesicular steatosis (black square). **G** TAA + Coq_{10} + LF group, showing minimal portal fibrosis infiltrated with few mononuclear cells (black arrows), and mild microvesicular steatosis (closed arrowhead), (H&E) staining (X:400, Bar = 50 µm**)**. **H** showing the histopathological score of the hepatic parenchyma in the different experimental groups (0–4), Mean ± SE, means with different letters indicate a significant difference ($P \leq 0.05$), SEM = standard error of the mean

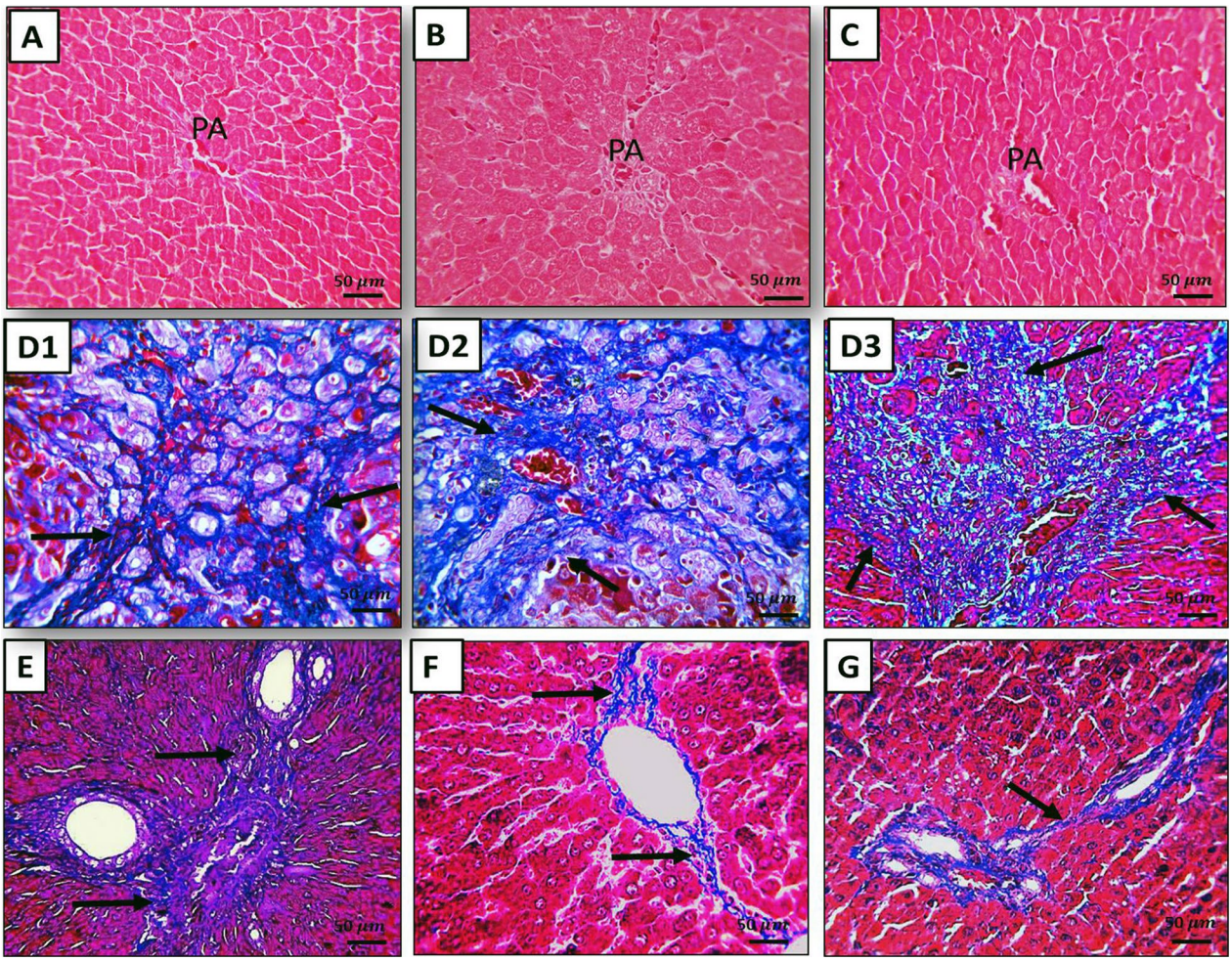

Fig. 5 Representative MTC stained hepatic micrographs from different experimental groups: **A**–**C** showing no collagen deposition in hepatic parenchyma around the portal areas (PA) in control, Coq_{10}, and LF groups, respectively. **D1**–**D3** TAA group, showing dense thick bluish fibrous septa dividing the hepatic parenchyma into separate nodules (arrows). **E** TAA + Coq_{10} group, revealing lower bluish collagen deposition in the portal area with short non-anastomosing fibrous extension and decrease in the deposition of the bluish collagen bundles (arrows). **F** TAA + LF, showing bluish portal thin anastomosing fibrous septa (arrows). **G** TAA + Coq_{10} + LF group, showing mild portal bluish collagen deposition very thin and very short non-anastomosing fibrous extension (arrow), (MTC) staining (X:400, Bar = 50µm)

endoplasmic reticulum besides intact tubular basement membrane (Fig. 8A). TAA induced marked ultrastructural damage including irregular thickened basement membrane, clumped rough endoplasmic reticulum, numerous lipid droplets, and lysosomes with autophagic vacuoles (Fig. 8B). The mitochondria were either shrunken clumped, or partially damaged with marked decrease in numbers. Conversely, the tubular micrographs of TAA + Coq_{10} group mostly appeared normal with few occasional mitochondrial clumping (Fig. 8C). TAA + LF group showed normal ultrastructures of nucleus, abundant intact mitochondria and rough endoplasmic reticulum (Fig. 8D). TAA + Coq_{10} + LF group showed minimal to mild enlarged nucleus with abundant autophagic vacuoles (Fig. 8E).

The TEM micrographs of the renal glomeruli from control, Coq_{10}, and LF groups showed normal capillary loops with a fenestrated endothelium and intact basement membrane (Fig. 9A). The foot processes of podocytes were regular in shape and connected with an intact filtration slit pores. TAA group exhibited intraluminal proliferated and fused endothelial cells, partially detached endothelium with loss of endothelial fenestration. The basement membrane showed multifocal

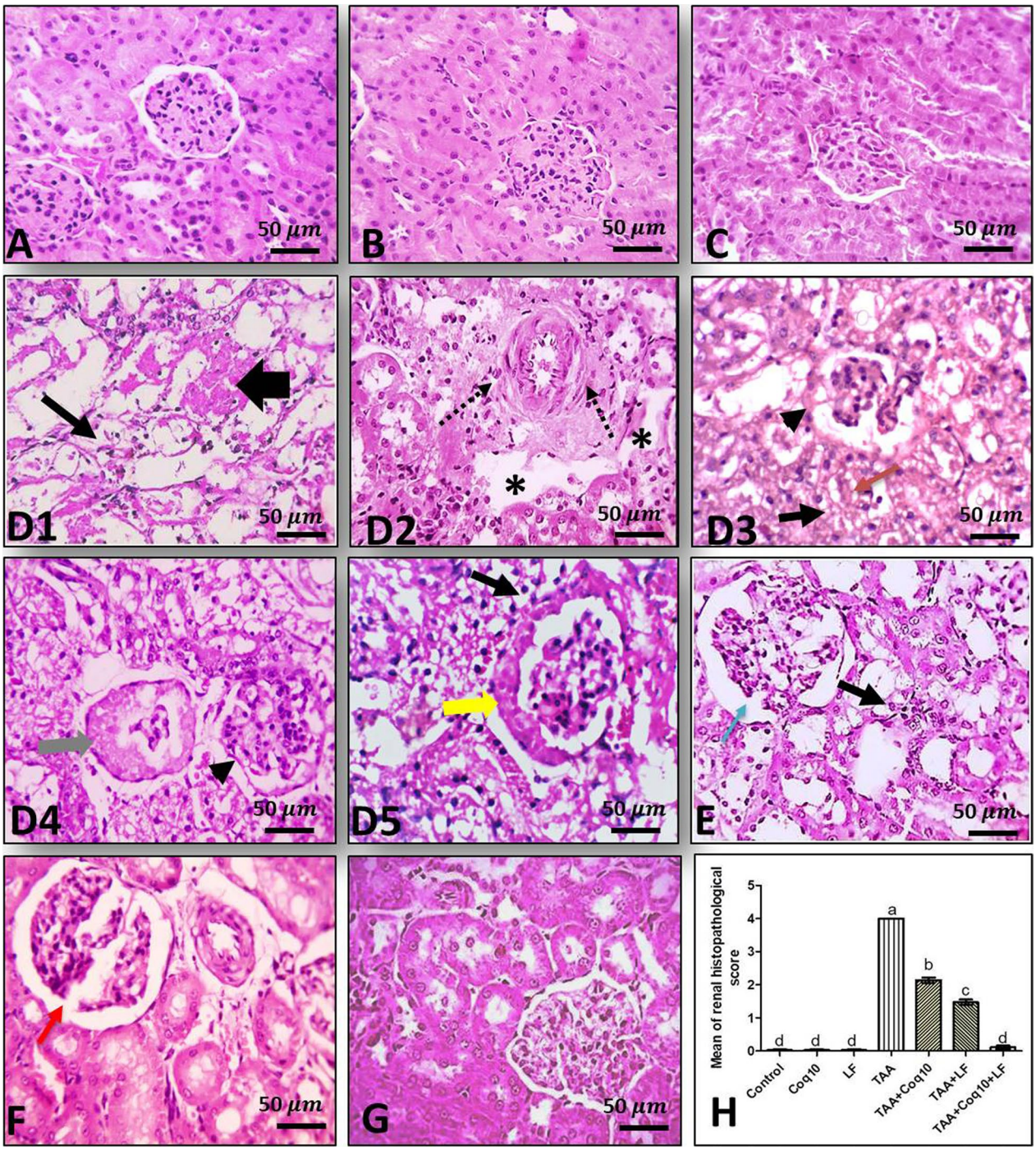

Fig. 6 Representative photomicrographs of renal cortex from different experimental groups: **A**–**C** showing normal renal parenchyma with normal glomeruli and renal tubules in control, Coq_{10}, and LF groups, respectively. **D1**–**D5** TAA group, showing diffuse hydropic degeneration (thin black arrows), and coagulative necrosis (thick black arrow) of tubular lining epithelium, perivascular fibrosis (dashed arrows), and edema (asterisks), besides cellular cast in the lumen of renal tubules (red arrow). The renal glomeruli are atrophied shrunken and necrotic (closed arrowheads), atrophied with thickened basement membrane (gray arrow), and crescent shape with thickened basement membrane (yellow arrow). **E** TAA + Coq_{10} group showing mild hydropic degeneration of tubular lining epithelium (black arrow) in few tubules and dilated Bowman's space (blue arrow). **F** TAA + LF group, showing dilated Bowman's space (red arrow). **G** TAA + Coq_{10} + LF group, showing an improved histological picture of tubules and glomeruli with normalized Bowman's space, (H&E) staining (X:400, Bar = 50 µm). **H** showing the histopathological score of the renal parenchyma in the different experimental groups, Mean ± SE, means with different letters indicate a significant difference at ($P \leq 0.05$), SEM = standard error of the mean

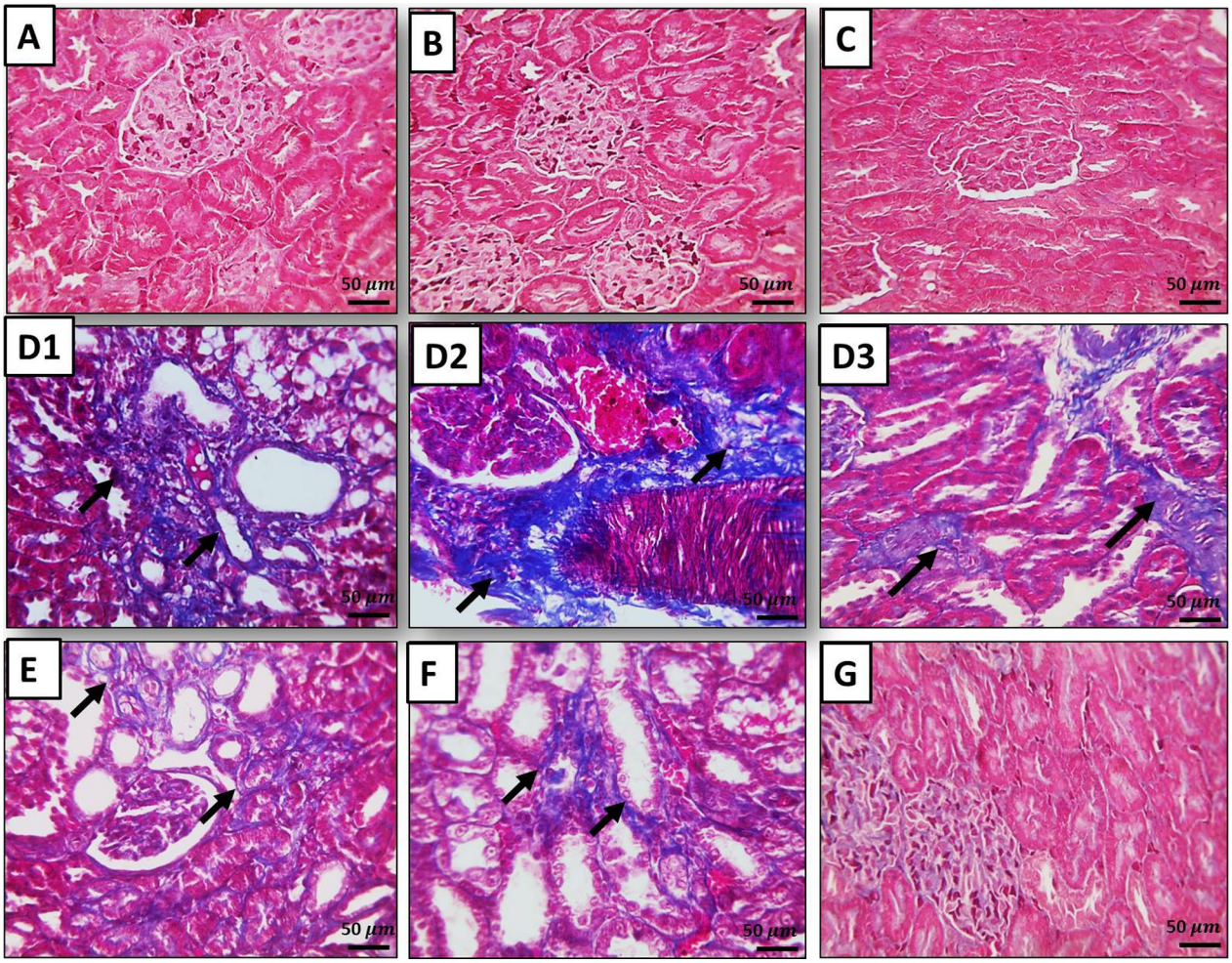

Fig. 7 Representative MTC stained renal micrographs from different experimental groups: **A**–**C** showing no collagen deposition in renal parenchyma in control, Coq_{10}, and LF groups, respectively. **D1**–**D3** TAA group, showing deposition of dense and thick bluish collagen bundles in the renal parenchyma (arrows). **E** TAA + Coq_{10} group, revealing mild fibrosis with decrease in the deposition of the bluish collagen in the renal parenchyma (arrows). **F** TAA + LF, showing minimal fibrosis with very low bluish collagen deposition in the renal parenchyma (arrows). **G** TAA + Coq_{10} + LF group, showing no collagen deposition in the renal parenchyma, (MTC) staining (X:400, Bar = 50μm)

segmental thickening and effacement of podocyte's foot processes with closure of the filtration slit pores (Fig. 9B). TAA + Coq_{10} showed partial loss of endothelial fenestration, focal irregularity of basement membrane and minimal fused podocytes (Fig. 9C). TAA + LF group showed regular structure of glomerular capillaries with fenestrated endothelium, intact basement membrane (Fig. 9D). The podocytes revealed numerous long processes with intact filtration pores. TAA + Coq_{10} + LF group showed minimal alterations in glomerular capillary represented by focal thickening of the basement membrane with a minimal fusion of podocyte's foot process. Moreover, the sections presented intact podocytes with normal foot processes and normal filtration slit (Fig. 9E).

3.5 Ubiquinone (Coq_{10}) and lactoferrin (LF) decrease TAA-induced secondary renal damage by down-regulating WNT4 gene expression

The analysis of WNT4 gene expression was applied to evaluate the efficacy of the WNT4 as a biomarker of TAA renal injury and investigate the protective ability of LF and Coq_{10} against TAA-induced renal damage.

The relative expression of WNT4 gene was significantly up-regulated in TAA group compared to the control group. However, the expression of WNT4 gene was significantly down-regulated in $TAA_{+}Coq_{10}$ and TAA + LF compared to TAA and the control groups. Meanwhile, a significant decrease in WNT4 expression was observed in the TAA + Coq_{10} + LF group compared to the TAA group with an insignificant increase from the control group (Fig. 10).

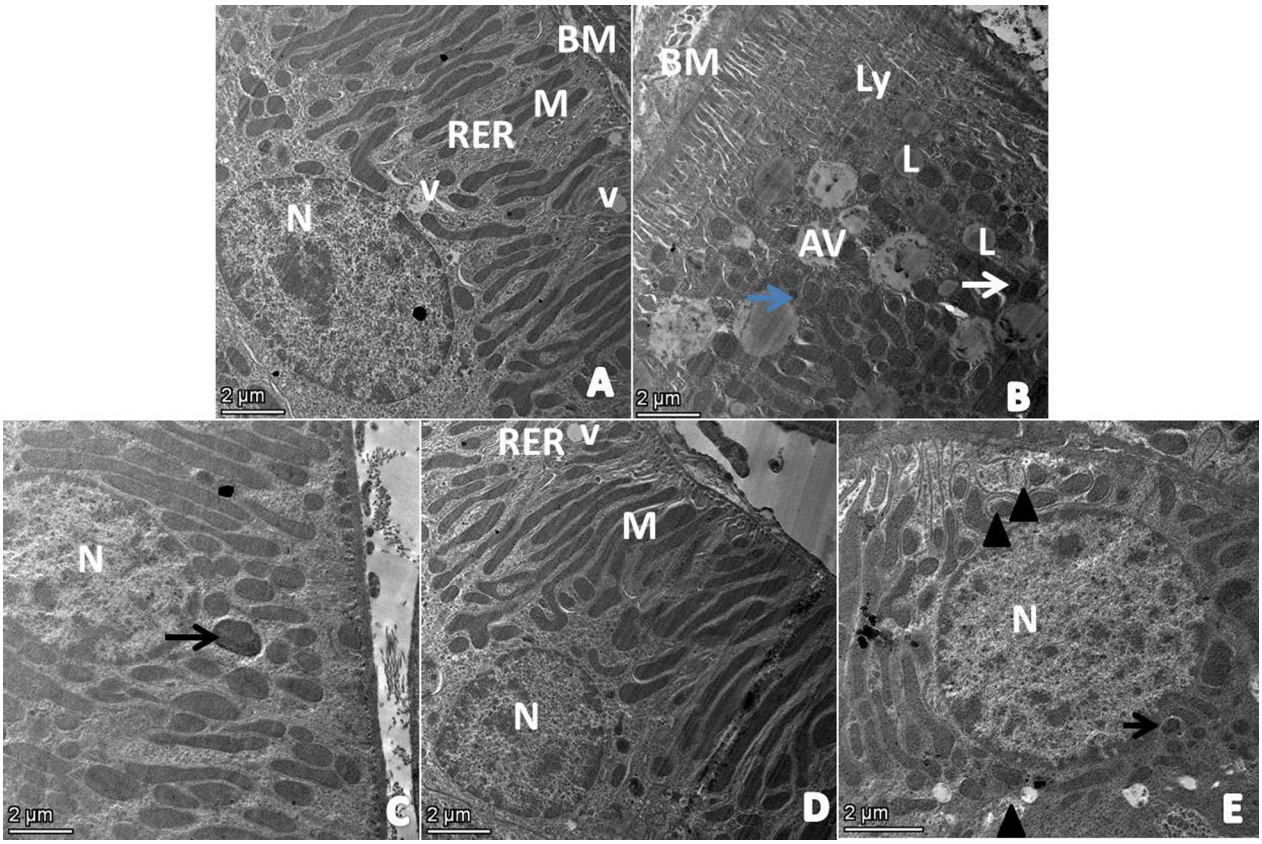

Fig. 8 Representative TEM micrographs of renal tubules from different experimental groups: **A** control group, showing normal ultrastructures of the nucleus with intact cytoplasmic mitochondria (M), rough endoplasmic reticulum (RER), and pinocytotic vesicle (V) besides intact tubular basement membrane (BM). **B** TAA group, showing thickened, irregular basement membrane (BM), clumped RER, numerous electron lucent lipid droplets (L), and autophagic vacuoles (AV) besides scattered electron-dense lysosome (LY). The mitochondria are shrunken and clumped (blue arrow), partially damaged mitochondria (white arrow) with marked decrease in number. **C** TAA + Coq_{10} group, showing mostly appeared normal ultrastructures with few alterations represented by occasional mitochondrial clumping with electron-dense matrix (black arrow). **D** TAA + LF showing normal ultrastructures of the nucleus, abundant intact mitochondria (M) and rough endoplasmic reticulum RER, few vesicles (V). **E** TAA + Coq_{10} + LF group, showing minimal to mild enlarged nucleus (N), few clumped mitochondria (thin arrow) with abundant membrane-bound organelles (autophagic vacuoles). Some bounded cytoplasmic organelles as mitochondria or granular particulate materials (arrowheads), most of them had clear phagocytic vacuoles Bar = 2 µm

4 Discussion

TAA is a powerful hepatotoxin with prolonged injury and recovery pattern [40]. In this study, TAA induced significant increase in the activities of ALT and AST in agreement with the work of Elnfarawy et al. [41]. Thus, ALT and AST are hepatic enzymes located in the cytoplasm of hepatocytes [42]. Hence, the elevated serum activities of ALT and AST indicating hepatic structural damage and impairment of the liver functions [43].

BUN is the first marker of renal injury, while SCr is the most reliable renal marker, and those parameters only increased when the bulk of renal functions is lost [44]. Our study showed a significant increase in the SCr activity and BUN level in TAA group suggesting severe renal injury [45]. The results are in consistent with the previous study that documented increase of SCr and BUN with TAA treatments in rats [46].

This study investigated the possible protective effects of Coq_{10}, LF and their combination on TAA-induced hepatorenal injury. The serum activities of ALT and AST in the TAA + Coq_{10} and TAA + LF groups were considerably decreased compared to TAA group after singular oral administration of Coq_{10} and LF. These results are concord with the previous studies [47, 48].

Additionally, TAA + Coq_{10} and TAA + LF groups showed significant decrease in the SCr and BUN compared to TAA group. These findings partially agreed with the previous studies on the therapeutic effects of Coq_{10} and LF in renal injury [49, 50]. Furthermore, our study showed that the combined oral administration of Coq_{10}

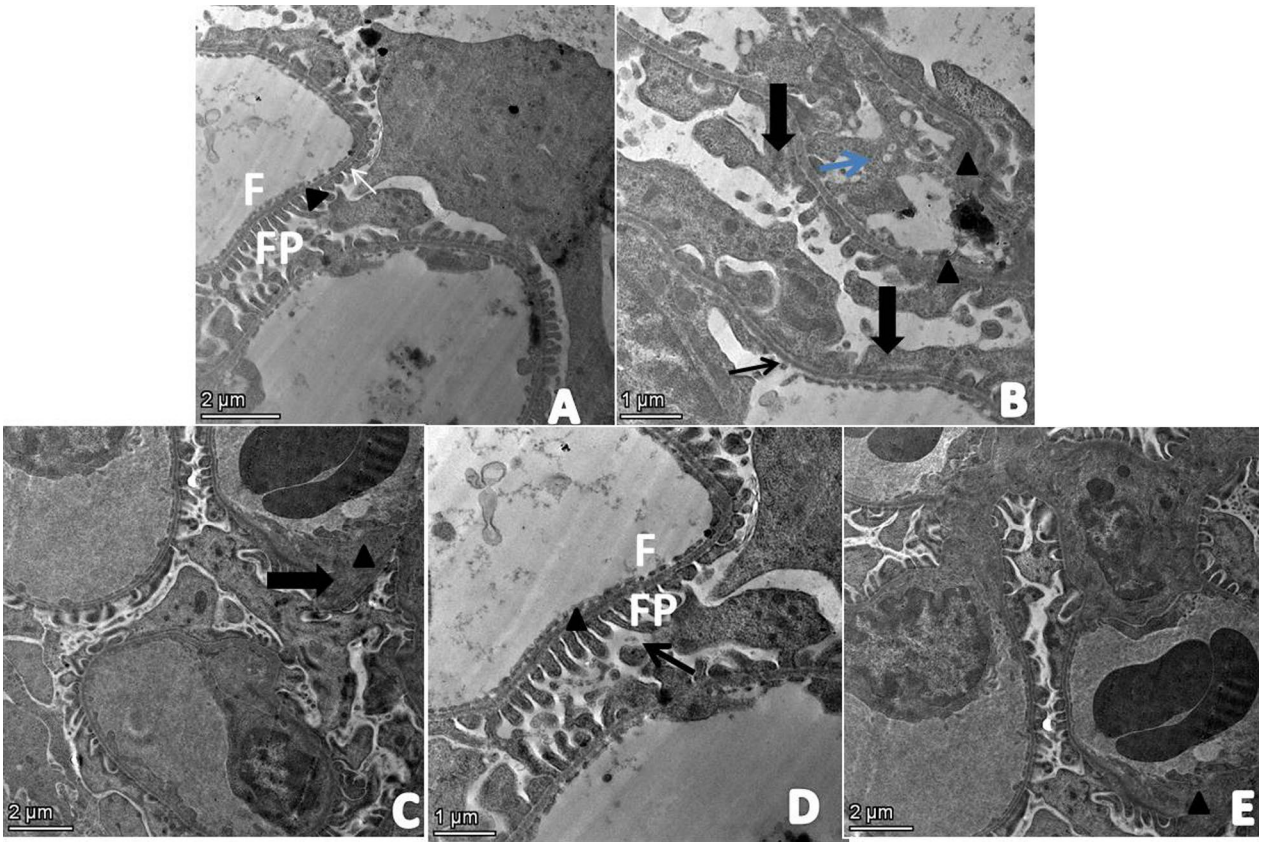

Fig. 9 Representative TEM micrographs of renal glomeruli from different experimental groups: **A** control group, glomerulus, showing normal capillary loops with a fenestrated endothelium (F), intact glomerular basement membrane (GBM) (arrowhead), regularly shaped foot process (FP) connected with an intact filtration slit (white arrow). **B** TAA group, showing intraluminal fused and proliferated endothelial cells (blue arrow), partially detached endothelium (thin black arrow) with loss of endothelial fenestration. The basement membrane showing a multifocal segmental thickening (arrowheads), and effacement of podocytes foot processes with closure of the filtration slit pores (thick arrows). **C** TAA + Coq_{10} group, showing partial loss of endothelial fenestration with focal irregularity of the GBM (arrowhead) and minimal fusion of podocytes (thick arrow). **D** TAA + LF group, showing regular structure of glomerular capillary with fenestrated endothelium (F), intact GBM(arrowhead), numerous long podocytes processes (FP) with intact filtration pores, occasionally detached podocyte processes (thin arrow). **E** TAA + Coq_{10} + LF group, showing minimal alterations in the glomerular capillary represented by focal thickening in GBM (arrowhead) with a minimal fusion of podocyte foot process. The section also showing intact podocyte with normal podocyte foot processes and normal filtration slit, Bar = 2 µm (A and C and E), Bar = 1 µm (B and D)

and LF in TAA + Coq_{10} + LF group maintained the serum activities of ALT, AST, SCr and BUN level into the normal values. To the best of our knowledge, our study could be the first study discussed the combined protective effects of Coq_{10} and LF against TAA hepatic and renal injury.

It was obvious that oxidative stress is the root of TAA toxicity, accrediting to TAA biotransformation, extensive production of ROS, surpassing the capacity of endogenous antioxidant protective mechanisms, resulting in oxidation of polyunsaturated fatty acids in biomembranes [51, 52]. In this study, TAA significantly increased the hepatic and renal concentrations of MDA, NOx as well as significantly decreased the hepatic and renal activities of SOD, CAT. These findings were similar to the earlier studies on TAA toxicity [6, 40]. Furthermore, the single administration of Coq_{10} and LF noticeably reduced oxidative stress. These findings are in consistent with the previous studies on the antioxidative activities of Coq_{10} and LF [53, 54].

The histopathological data are pointed to the protective effects of Coq_{10} and LF against TAA-induced hepatorenal injury. TAA induced severe hepatic damage signified by cirrhosis, inflammation, steatosis, apoptosis hyperchromatia, and mitotic figures in the hepatic parenchyma. In addition, the renal parenchyma showed fibrosis, necrosis of tubular lining epithelium, atrophy, and necrosis of glomeruli with thickened basement membrane in TAA

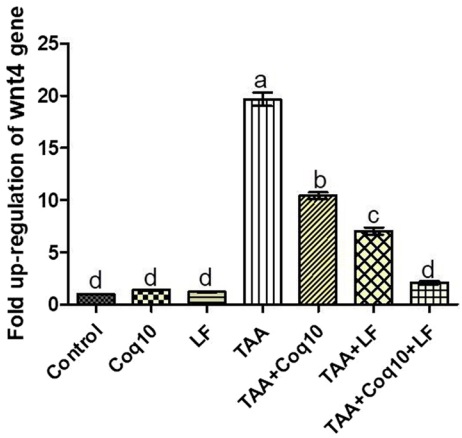

Fig. 10 Relative expression of the WNT4 gene by RT-PCR in different studied groups: mean ± SEM, means with different letters indicate a significant difference ($P \leq 0.05$), SEM = standard error of the mean

group. These histopathological observations were in accordance with the biochemical findings and parallel to the findings of previous studies [55, 56]. Our histopathological analyses showed that the hepatic and renal lesions were decreased in groups exposed to TAA and treated with both/or Coq_{10} LF compared to TAA group.

The ultrastructural findings confirmed the histopathological data and illustrated the mechanism of heptorenal injury. TAA induced severe ultrastructural damage of the renal tubular epithelium, represented in clumped, dense, or fragmented mitochondria, besides degenerated and fragmented rough endoplasmic reticulum. Mitochondria are the cellular house of energy [57]. Therefore, the mitochondrial damage indicated cellular oxidative damage [58]. These findings resembled the ultrastructural findings of amoxicillin nephrotoxicity in mice [59]. In the context of this, the renal glomeruli showed thickening of the glomerular basement membrane, damage in the glomerular endothelium and effacement of podocyte foot process with closure filtration slit pores. The podocytes are highly specialized cells that play the main role in the glomerular filtration barrier [60]. They are finely organized to maintain the slit membrane of the glomerulus[61]. The previous studies revealed that the structural loss of the podocytes is represented by the effacement of their foot processes [62]. The injury of podocytes and glomerular endothelium are incorporated in glomerulosclerosis which considered the hallmark of chronic kidney disease [61].

The mechanism of TAA-induced hepatorenal renal injury secondary to liver cirrhosis were not clarified before. We suggested that TAA active metabolites induced marked oxidative stress resulted in marked hepatic injury and associated with fibrosis and cirrhosis. The deposition of the fibrous tissue caused marked portal hypertension and increased the intrahepatic vascular resistance [63]. Also, the oxidative stress enhanced the release of the vasodilators as NOx in the splanchinic circulation resulted in splanchinic vasodilatation [64]. The portal hypertension together with the splanchinic vasodilatation caused decrease in the effective blood pressure and decrease in the renal blood flow [65]. The decreased renal blood flow resulted in damage of the glomerular endothelium and injury of the podocytes with fusion or effacement of their foot process, causing thickening of the glomerular basement membrane. The damaged endothelium and the thickening of the glomerular basement membrane resulted in closure of the filtration slit and decrease of the glomerular filtration. This interfered with the renal reperfusion, causing renal fibrosis and renal failure.

The renal TEM of TAA + Coq_{10} and TAA + LF groups showed minimal mitochondrial alterations in the renal tubules and minimal damage to the glomerular endothelium and podocytes. TAA + Coq_{10} + LF group showed marked morphological improvements of the renal tubules including minimal focal thickening of the glomerular basement besides intact podocytes with normal foot processes and normal filtration slit. To the best of our knowledge, this is the first study demonstrated the single and combined ultrastructural protective activities of Coq_{10} and LF in renal parenchyma.

The injury of the mature kidney triggers a sum of developmental genes including WNT4 [66]. To verify that the expression of WNT4 related to tubular damage, we detected significant up-regulation of WNT4 gene in TAA group, indicating renal injury. As previously mentioned the expression of WNT4 elevated in the pathogenesis of podocyte injury and renal tubular damage [67, 68]. This illustrates the relation between the expression of this gene and the ultrastructural findings and clarifies the mechanism of TAA-induced renal damage. Additionally, its expression is increased in cases of chronic renal injury [66]. This renal ischemia is secondary to hepatic cirrhosis, splanchnic vasodilatation and consecutive renal vasoconstriction [69, 70]. Hence, WNT4 gene could be more helpful for detecting renal ischemia and thus renal damage [71]. In contrast, the expression of WNT4 gene was significantly decreased in TAA + Coq_{10} and TAA + LF groups compared to TAA group, and was significantly increased compared to control group. Meanwhile, TAA + Coq_{10} + LF group recorded significant down-regulation in the expression of WNT4 compared to TAA group without significant increase from the control group. These findings speculated the protective effects of LF and Coq_{10} against TAA-induced secondary renal damage. As far we know, the influence of TAA, Coq_{10},

and LF on the expression of WNT4 gene has not been discussed before.

Taken together, our data showed the protective effect of Coq_{10} and LF against TAA-induced hepatorenal injury by improving hepatrorenal functions, histopathology and ultrastructural alterations, reducing oxidative stress marker and down-regulating the WNT4 gene. Additionally, the combined protective effect of both Coq_{10} and LF was more effective than the single effect of Coq_{10} or LF. This assumed to the synergetic effects of the antioxidative effect of Coq_{10} and the antioxidative, antiinflammatory and the antifibrotic effects of LF. Hence, the combination of Coq_{10} and LF could be established as a potential protective regimen against hepatorenal damage.

5 Conclusion

In conclusion, (a) the ultrastructural findings clarified the mechanism of TAA-induced hepatorenal injury; (b) the WNT4 gene expression confirmed the mechanism of TAA hepatorenal injury; Coq_{10} and LF biochemically and histopathologically diminished TAA-induced hepatic and renal damage; (c) Coq_{10} and LF significantly inhibited oxidative stress biomarkers (MDA and NOx) and significantly increased the antioxidative systems (SOD and CAT); (d) Coq_{10} and LF significantly decreased hepatic fibrosis, cirrhosis, apoptosis, steatosis, and inflammation; and (e) the combination between Coq_{10} and LF was more effective and powerful than Coq_{10} and LF alone. Based on all the findings, Coq_{10} and LF could be a potential preventing regimen against hepatic and renal injury.

Abbreviations

ALT	Alanine aminotransferase
AST	Aspartate transaminase
AV	Autophagic vacuoles
BM	Basement membrane
CAT	Catalase
Coq_{10}	Coenzyme q_{10}
F	Fenesterated endothelium
FP	Foot processes
GBM	Glomerular basement membrane
H&E	Hematoxylin and eosin
L	Lipid particles
LF	Lactoferrin
LY	Lysosome
M	Mitochondria
MDA	Malondialdhyde
MTC	Masson's trichrome
N	Nucleus
NOx	Nitric oxide
V	Pinocytotic vesicle
PA	Portal area
RER	Rough endoplasmic reticulum
ROS	Reactive oxygen species
RT-PCR	Reverse transcription polymerase chain reaction
SEM	Standard error of the mean
SOD	Superoxide dismutase
TAA	Thioacetamide

Acknowledgements
The authors express their cordial thanks to Prof. Dr. Mohammed Al-Adl, Professor of Biochemistry, Faculty of Veterinary Medicine, Mansoura University and Dr. Reham Karam, Lecturer of Virology, Faculty of Veterinary Medicine, Mansoura University, for their help in finishing the gene expression part.

Author contributions
All authors (AE, WA, Il, and SA) carried out the experiment. AE designed the experiment. SA wrote the material and method, the results, and the discussion. Il wrote the introduction part and wrote the results of electron microscope. WA carried out the histopathological examination and statistically analyzed data. SA carried out the experiment and the gene expression procedures, and participated in writing all parts of the manuscript. AE, WA, and Il revised and approved the manuscript.

Funding
This research did not receive any specific grant from funding agencies in the public, commercial, or not-for-profit sectors.

Availability of data and materials
The data that support the findings of this study are available on request from the corresponding author.

Declarations

Ethics approval
The rats of this experiment were obtained from the Animal Experimental Center, Faculty of Veterinary Medicine, Zagazig University, Egypt. The experimental techniques were carried out at the Pathology Lab, Faculty of Veterinary Medicine, Mansoura University. This research is approved by the Medical Research Ethics Committee of Mansoura University at the April 11, 2021, Code No, Ph.D, 85. The guidelines of the Medical Research Ethics Committee of Mansoura University are following the ARRIVE guidelines.

Consent for publication
Not applicable.

Competing interests
The author(s) declared no potential conflicts of interest with respect to the research, authorship, and/or publication of this article.

Author details
[1]Department of Pathology, Faculty of Veterinary Medicine, Mansoura University, Mansoura 35516, Egypt.

Received: 17 July 2023 Accepted: 2 April 2024
Published online: 03 May 2024

References

1. Liu T, Wang X, Karsdal MA, Leeming DJ, Genovese F (2012) Molecular serum markers of liver fibrosis. Biomarker Insights 7:105–117
2. Huelin P, Piano S, Solà E, Stanco M, Solé C, Moreira R, Pose E, Fasolato S, Fabrellas N, De Prada G (2017) Validation of a staging system for acute kidney injury in patients with cirrhosis and association with acute-on-chronic liver failure. Clin Gastroenterol Hepatol 15:438–445
3. Angeli P, Ginès P, Wong F, Bernardi M, Boyer TD, Gerbes A, Moreau R, Jalan R, Sarin SK, Piano S (2015) Diagnosis and management of acute kidney injury in patients with cirrhosis: revised consensus recommendations of the International Club of Ascites. Gut 64:531–537
4. Puoti C (2012) The use of vasoconstrictors in patients with liver cirrhosis: how, when, why. Clin Manag 6:105–115
5. Varga ZV, Erdelyi K, Paloczi J, Cinar R, Zsengeller ZK, Jourdan T, Matyas C, Nemeth BT, Guillot A, Xiang X (2018) Disruption of renal arginine metabolism promotes kidney injury in hepatorenal syndrome in mice. Hepatol 68:1519–1533

6. Ghosh S, Sarkar A, Bhattacharyya S, Sil PC (2016) Silymarin protects mouse liver and kidney from thioacetamide induced toxicity by scavenging reactive oxygen species and activating PI3K-Akt pathway. Front Pharmacol 7:481
7. Kaur V, Kumar M, Kaur P, Kaur S, Singh AP, Kaur S (2017) Hepatoprotective activity of Butea monosperma bark against thioacetamide-induced liver injury in rats. Biomed Pharmacother 89:332–341
8. Matsuo M, Murata S, Hasegawa S, Hatada Y, Ohtsuka M, Taniguchi H (2020) Novel liver fibrosis model in *Macaca fascicularis* induced by thioacetamide. Sci Rep 10:1–7
9. Zargar S, Wani TA, Alamro AA, Ganaie MA (2017) Amelioration of thioacetamide-induced liver toxicity in Wistar rats by rutin. Int J Immunopathol pharmacol 30:207–214
10. Begum Q, Noori S, Mahboob T (2011) Antioxidant effect of sodium selenite on thioacetamide-induced renal toxicity. Pak J Biochem Mol Biol 44:21–26
11. Silva FG (2004) Chemical-induced nephropathy: a review of the renal tubulointerstitial lesions in humans. Toxicol Pathol 32:71–84
12. Liu Z, Liu X, Yang Q, Yu L, Chang Y, Qu M (2020) Neutrophil membrane-enveloped nanoparticles for the amelioration of renal ischemia-reperfusion injury in mice. Acta Biomater 104:158–166
13. Chassot A-A, Bradford ST, Auguste A, Gregoire EP, Pailhoux E, De Rooij DG, Schedl A, Chaboissier M-C (2012) WNT4 and RSPO1 together are required for cell proliferation in the early mouse gonad. Development 139:4461–4472
14. Surendran K, Mccaul SP, Simon TC (2002) A role for Wnt-4 in renal fibrosis. Am J Physiol Renal Physiol 282:F431–F441
15. Molyneux SL, Florkowski CM, George PM, Pilbrow AP, Frampton CM, Lever M, Richards AM (2008) Coenzyme Q10: an independent predictor of mortality in chronic heart failure. J Am Coll Cardiol 52:1435–1441
16. Bentinger M, Brismar K, Dallner G (2007) The antioxidant role of coenzyme Q. Mitochondrion 7:S41–S50
17. Munier-Lehmann HLN, Lucas-Hourani M, Guillou S, Helynck O, Zanghi G, Noel A, Tangy FDR, Vidalain P-O, Janin YL (2015) Original 2-(3-alkoxy-1 H-pyrazol-1-yl) pyrimidine derivatives as inhibitors of human dihydroorotate dehydrogenase (DHODH). J Med Chem 58:860–877
18. Galeshkalami NS, Abdollahi M, Najafi R, Baeeri M, Jamshidzade A, Falak R, Gholami MD, Hassanzadeh G, Mokhtari T, Hassani S (2019) Alpha-lipoic acid and coenzyme Q10 combination ameliorates experimental diabetic neuropathy by modulating oxidative stress and apoptosis. Life Sci 216:101–110
19. Abdeen A, Abdelkader A, Elgazzar D, Aboubakr M, Abdulah OA, Shoghy K, Abdel-Daim M, El-Serehy HA, Najda A, El-Mleeh A (2020) Coenzyme Q10 supplementation mitigates piroxicam-induced oxidative injury and apoptotic pathways in the stomach, liver, and kidney. Biomed Pharmacother 130:110627
20. Siqueiros-Cendón T, Arévalo-Gallegos S, Iglesias-Figueroa BF, García-Montoya IA, Salazar-Martínez J, Rascón-Cruz Q (2014) Immunomodulatory effects of lactoferrin. Acta Pharmacol Sin 35:557–566
21. Öztafl YE, Özgünefl N (2005) Lactoferrin: a multifunctional protein. Adv Mol Med 1:149–154
22. González-Chávez SA, Arévalo-Gallegos S, Rascón-Cruz Q (2009) Lactoferrin: structure, function and applications. Int J Antimicrob Agents 33(301):e1–e8
23. Hessin A, Hegazy R, Hassan A, Yassin N, Kenawy S (2015) Lactoferrin enhanced apoptosis and protected against thioacetamide-induced liver fibrosis in rats. Maced J Sci 3(2):195
24. Said RS, Mohamed HA, Kamal MM (2019) Coenzyme Q10 mitigates ionizing radiation-induced testicular damage in rats through inhibition of oxidative stress and mitochondria-mediated apoptotic cell death. Toxicol Appl Pharmacol 383:114780
25. Hegazy R, Salama A, Mansour D, Hassan A (2016) Renoprotective effect of lactoferrin against chromium-induced acute kidney injury in rats: involvement of IL-18 and IGF-1 inhibition. PLoS ONE 11:e0151486
26. Abdou S, Taha N, Lebda M, Elhoffy H, Hashem A (2019) Role of melatonin in preventing thioacetamide-induced liver injury in rats. Damanhour J Vet Sci 1:19–21
27. Reitman S, Frankel S (1957) A colorimetric method for the determination of serum glutamic oxalacetic and glutamic pyruvic transaminases. Am J Clin Pathol 28:56–63
28. Murray R (1984) Creatinine. In: Kaplan LA, Pesce AJ (eds) Clinical chemistry: theory, analysis and correlation. CV Mosby Company, St. Louis, pp 1247–1253
29. Nishikimi M, Rao NA, Yagi K (1972) The occurrence of superoxide anion in the reaction of reduced phenazine methosulfate and molecular oxygen. Biochem Biophys Res Commun 46:849–854
30. Kei S (1978) Serum lipid peroxide in cerebrovascular disorders determined by a new colorimetric method. Clin Chim Acta 90:37–43
31. Bancroft J, Gamble M (2008) Theory and practice of histological techniques, 7th ed., Churchill Livingstone London. In: Elsevier health sciences. UK, pp 73–138
32. Kleiner DE, Brunt EM, Van Natta M, Behling C, Contos MJ, Cummings OW, Ferrell LD, Liu YC, Torbenson MS, Unalp-Arida A (2005) Design and validation of a histological scoring system for nonalcoholic fatty liver disease. Hepatol 41:1313–1321
33. Zheng Z, Schmidt-Ott KM, Chua S, Foster KA, Frankel RZ, Pavlidis P, Barasch J, D'agati VD, Gharavi AG (2005) A Mendelian locus on chromosome 16 determines susceptibility to doxorubicin nephropathy in the mouse. Proc Nati Acad Sci 102:2502–2507
34. Bozzola JJ, Russell LD (1999) Electron microscopy: principles and techniques for biologists. Jones & Bartlett Learning, Boston, p 670
35. Terada Y, Tanaka H, Okado T, Shimamura H, Inoshita S, Kuwahara M, Sasaki S (2003) Expression and function of the developmental gene Wnt-4 during experimental acute renal failure in rats. J Am Soc Nephrol 14:1223–1233
36. Banni M, Messaoudi I, Said L, El Heni J, Kerkeni A, Said K (2010) Metallothionein gene expression in liver of rats exposed to cadmium and supplemented with zinc and selenium. Archiv Environ Contam Toxicol 59:513–519
37. Yuan JS, Reed A, Chen F, Stewart CN (2006) Statistical analysis of real-time PCR data. BMC Bioinform 7:1–12
38. Brown AM (2005) A new software for carrying out one-way ANOVA post hoc tests. Comput Methods Programs Biomed 79:89–95
39. Motulsky HJ (2007) Prism 5 statistics guide. GraphPad Software Inc., San Diego
40. El Awdan SA, Abdel Rahman RF, Ibrahim HM, Hegazy RR, El Marasy SA, Badawi M, Arbid MS (2019) Regression of fibrosis by cilostazol in a rat model of thioacetamide-induced liver fibrosis: Up regulation of hepatic cAMP, and modulation of inflammatory, oxidative stress and apoptotic biomarkers. PLoS ONE 14(5):e0216301
41. Elnfarawy AA, Nashy AE, Abozaid AM, Komber IF, Elweshahy RH, Abdelrahman RS (2021) Vinpocetine attenuates thioacetamide-induced liver fibrosis in rats. Hum Exp Toxicol 40:355–368
42. Ramaiah SK (2007) A toxicologist guide to the diagnostic interpretation of hepatic biochemical parameters. Food Chem Toxicol 45:1551–1557
43. Domitrović R, Škoda M, Marchesi VV, Cvijanović O, Pugel EP, Štefan MB (2013) Rosmarinic acid ameliorates acute liver damage and fibrogenesis in carbon tetrachloride-intoxicated mice. Food Chem Toxicol 51:370–378
44. Borges LP, Borges VC, Moro AV, Nogueira CW, Rocha JBT, Zeni G (2005) Protective effect of diphenyl diselenide on acute liver damage induced by 2-nitropropane in rats. Toxicol 210:1–8
45. Bonventre JV (2008) Kidney Injury Molecule-1 (KIM-1): a specific and sensitive biomarker of kidney injury. Scand J Clin Lab Invest 68:78–83
46. Alomar MY (2020) Physiological and histopathological study on the influence of Ocimum basilicum leaves extract on thioacetamide-induced nephrotoxicity in male rats. Saudi J Biol Sci 27:1843–1849
47. AaS S, Shahin MI, Kelada NA (2017) Hepatoprotective effect of taurine and coenzyme Q10 and their combination against acrylamide-induced oxidative stress in rats. Trop J Pharm Res 16:1849–1855
48. Farid AS, El Shemy MA, Nafie E, Hegazy AM, Abdelhiee EY (2021) Anti-inflammatory, anti-oxidant and hepatoprotective effects of lactoferrin in rats. Drug Chem Toxicol 44:286–293
49. Kimoto Y, Nishinohara M, Sugiyama A, Haruna A, Takeuchi T (2013) Protective effect of lactoferrin on cisplatin-induced nephrotoxicity in rats. J Vet Med Sci 75:159–164
50. Carrasco J, Anglada FJ, Campos JP, Muntané J, Requena MJ, Padillo J (2014) The protective role of coenzyme Q10 in renal injury associated with extracorporeal shockwave lithotripsy: a randomised, placebo-controlled clinical trial. BJU Int 113:942–950
51. Ansil PN, Nitha A, Prabha SP, Wills PJ, Jazaira V, Latha MS (2011) Protective effect of *Amorphophallus campanulatus* (Roxb.) Blume. tuber against

thioacetamide induced oxidative stress in rats. Asian Pac J Trop Med 4:870–877
52. Shirin H, Sharvit E, Aeed H, Gavish D, Bruck R (2013) Atorvastatin and rosuvastatin do not prevent thioacetamide induced liver cirrhosis in rats. World J Gastroenterol 19:241
53. Hsu Y-H, Chiu I-J, Lin Y-F, Chen Y-J, Lee Y-H, Chiu H-W (2020) Lactoferrin contributes a renoprotective effect in acute kidney injury and early renal fibrosis. Pharm 12:434
54. Huynh K, Kiriazis H, Du X-J, Love J, Jandeleit-Dahm K, Forbes J, Mcmullen JR, Ritchie RH (2012) Coenzyme Q 10 attenuates diastolic dysfunction, cardiomyocyte hypertrophy and cardiac fibrosis in the db/db mouse model of type 2 diabetes. Diabetologia 55:1544–1553
55. Ahmad A, Alkreathy HM (2018) Comparative biochemical and histopathological studies on the efficacy of metformin and Nigella sativa oil against thioacetamide-induced acute hepatorenal damage in rats. Biomed Res 29:3106–3116
56. Su W, Tai Y, Tang S-H, Ye Y-T, Zhao C, Gao J-H, Tuo B-G, Tang C-W (2020) Celecoxib attenuates hepatocyte apoptosis by inhibiting endoplasmic reticulum stress in thioacetamide-induced cirrhotic rats. World J Gastroenterol 26:4094
57. Ernster L, Schatz G (1981) Mitochondria: a historical review. The J Cell Biol 91:227s–255s
58. Faa G, Ambu R, Congiu T, Costa V, Ledda-Columbano G, Coni P, Curto M, Giacomini L, Columbano A (1992) Early ultrastructural changes during thioacetamide-induced apoptosis in rat liver. J Submicrosc Cytol Pathol 24:417–424
59. Sabry SA, Rashad HI, Shahin MA (2020) Histopathological and ultrastructural alterations in the renal cortex of albino mice foetuses induced by beta-lactam Antibiotic'Amoxicillin'. Egypt J Hosp Med 81:2340–2351
60. Deegens JK, Dijkman HB, Borm GF, Steenbergen EJ, Van Den Berg JG, Weening JJ, Wetzels JF (2008) Podocyte foot process effacement as a diagnostic tool in focal segmental glomerulosclerosis. Kidney Int 74:1568–1576
61. Taneda S, Honda K, Ohno M, Uchida K, Nitta K, Oda H (2015) Podocyte and endothelial injury in focal segmental glomerulosclerosis: an ultrastructural analysis. Virchows Arch 467:449–458
62. van den Bergh Weerman MA, Assmann KJ, Weening JJ, Florquin S (2004) Podocyte foot process effacement is not correlated with the level of proteinuria in human glomerulopathies. Kidney Int 66(5):1901–1906
63. De Franchis R, Primignani M (2001) Natural history of portal hypertension in patients with cirrhosis. Clin Liver Dis 5:645–663
64. Abraldes JG, Rodríguez-Vilarrupla A, Graupera M, Zafra C, García-Calderó H, García-Pagán JC, Bosch J (2007) Simvastatin treatment improves liver sinusoidal endothelial dysfunction in CCl4 cirrhotic rats. J Hepatol 46:1040–1046
65. Simonetto DA, Gines P, Kamath PS (2020) Hepatorenal syndrome: pathophysiology, diagnosis, and management. BMJ Brit Med J 370:m2687
66. Kiewisz J, Skowronska A, Winiarska A, Pawlowska A, Kiezun J, Rozicka A, Perkowska-Ptasinska A, Kmiec Z, Stompor T (2019) WNT4 expression in primary and secondary kidney diseases: dependence on staging. Kidney Blood Press Res 44:200–210
67. Dai C, Stolz DB, Kiss LP, Monga SP, Holzman LB, Liu Y (2009) Wnt/β-catenin signaling promotes podocyte dysfunction and albuminuria. J Am Soc Nephrol 20:1997
68. Dirocco DP, Kobayashi A, Taketo MM, Mcmahon AP, Humphreys BD (2013) Wnt4/β—Catenin signaling in medullary kidney myofibroblasts. J Am Soc Nephrol 24:1399
69. Møller-Kristensen M, Wang W, Ruseva M, Thiel S, Nielsen S, Takahashi K, Shi L, Ezekowitz A, Jensenius J, Gadjeva M (2005) Mannan-binding lectin recognizes structures on ischaemic reperfused mouse kidneys and is implicated in tissue injury. Scand J Immunol 61:426–434
70. Hwang I, Seo E-Y, Ha H (2009) Wnt/β-catenin signaling: a novel target for therapeutic intervention of fibrotic kidney disease. Arch Pharm Res 32:1653–1662
71. Zhao S-L, Wei S-Y, Wang Y-X, Diao T-T, Li J-S, He Y-X, Yu J, Jiang X-Y, Cao Y, Mao X-Y (2016) Wnt4 is a novel biomarker for the early detection of kidney tubular injury after ischemia/reperfusion injury. Sci Rep 6:32610

Publisher's Note